Self-Consistent Model for Planar Ferrite Growth in Fe-C-X Alloys

H.S. ZUROB, D. PANAHI, C.R. HUTCHINSON, Y. BRECHET, and G.R. PURDY

A self-consistent model for non-partitioning planar ferrite growth from alloyed austenite is presented. The model captures the evolution with time of interfacial contact conditions for substitutional and interstitial solutes. Substitutional element solute drag is evaluated in terms of the dissipation of free energy within the interface, and an estimate is provided for the rate of buildup of the alloying element "spike" in austenite. The transport of the alloying elements within the interface region is modeled using a discrete-jump model, while the bulk diffusion of C is treated using a standard continuum treatment. The model is validated against ferrite precipitation and decarburization kinetics in the Fe-Ni-C, Fe-Mn-C, and Fe-Mo-C systems.

I. INTRODUCTION

THE influence of alloying elements on the kinetics of ferrite growth in steel has been the subject of investigation and debate for over a century. The roots of the problem lie almost entirely in the differences in mobilities of the substitutional and interstitial solutes (*e.g.*, Mn and C) in steel. In the binary Fe-C system, the relaxation times of ferrite growth are necessarily related to the diffusion of carbon, either in austenite or in ferrite or in the interface joining them. Thus, for example, in the isothermal growth of planar grain boundary ferrite from supersaturated austenite, one finds that a local equilibrium model of the kind initially proposed by Zener[1] gives an adequate first order representation of the thickening kinetics. In contrast, it has been recognized for more than half a century that the simple extension of the Zener model to the thickening of grain boundary ferrite allotriomorphs in ternary and higher order iron alloys is not so straightforward. The instinctive choice of tie-line which includes the bulk composition does not yield a satisfactory solution, as the two solute mass balances cannot be simultaneously satisfied. The selection of the appropriate interfacial tie-line then becomes a part of the solution of the growth problem, as pointed out for example by Kirkaldy[2] and Hillert,[3] who examined solutions of the three component diffusion equations under the assumption of full interfacial local equilibrium. Indeed, the interfacial tie-line that does satisfy both solute mass balances is one that permits negligible partitioning of the substitutional solute (X) and which therefore forms unpartitioned ferrite of the bulk composition, as shown in Figure 1. On this reasoning, one expects that ferrite growth will be fast and limited only by the diffusion of carbon. The same argument holds for all initial austenite compositions within the "Local equilibrium, negligible-partition" (LE-NP) boundary.

A similar approach to the selection of the local equilibrium interfacial tie-line for bulk austenite compositions above the LE-NP boundary dictates that the transformation product should be accompanied by the long-range redistribution of the substitutional solute, X; the rates of growth would then be dictated by the rate of diffusion of this component and would then be much slower than those within the envelope. This argument has been expressed in a different language by Hillert,[3] Purdy *et al.*,[4] and Coates.[5]

An alternative (partial) local equilibrium boundary condition, "Paraequilibrium," PE, was first proposed by Hultgren[6] and later developed by Hillert.[3] In this (conceptual) state, the substitutional component (X) is considered essentially inert and undisturbed by the passage of the interface. The mobile interstitial component (C) is permitted to come to a constrained local equilibrium defined by the equality of chemical potentials

$$\mu_C^\alpha = \mu_C^\gamma \tag{1}$$

while the substitutional solute (X) and the solvent (Fe) must suffer chemical potential differences across the moving interface[7]:

$$\left(\mu_{Fe}^\alpha - \mu_{Fe}^\gamma\right)x_{Fe} = \left(\mu_X^\gamma - \mu_X^\alpha\right)x_X \tag{2}$$

For the ternary case, these assumptions constrain the PE tie-lines to coincide with carbon component rays (lines radiating from the carbon corner of the ternary isotherm). This expression can be generalized to any number of interstitial and substitutional components.

Two comments are in order at this point. First, since the PE and LE-NP boundary conditions are computed from purely thermodynamic data, they represent cases

H.S. ZUROB, Associate Professor, D. PANAHI, Graduate Student, and G.R. PURDY, Professor, are with the Department of Materials Science and Engineering, McMaster University, Hamilton, ON, Canada. Contact e-mail: zurobh@mcmaster.ca C.R. HUTCHINSON, Associate Professor, is with the Department of Materials Engineering, Monash University, Clayton, 3800 VIC, Australia. Y. BRECHET, Professor, is with the SIMAP, Institute National Polytechnique de Grenoble, St Martin D'Hères 38402, Grenoble, France.
Manuscript submitted June 30, 2012.
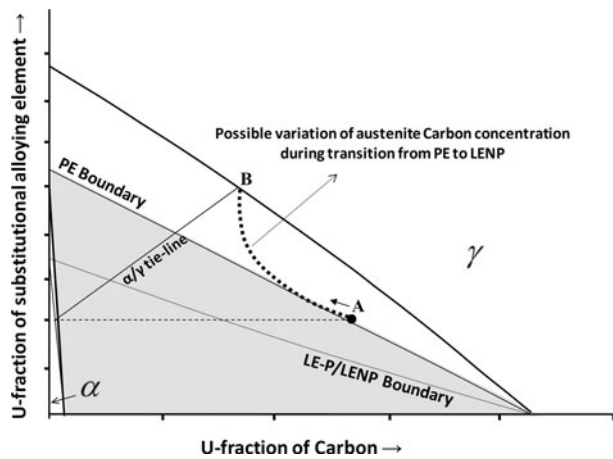Article published online October 24, 2012

Fig. 1—Isothermal section-showing PE and LENP limits as well as the interfacial compositions traced in transition models.

which may or may not be realized in practice. They are not to be taken a priori as bases for models that purport to predict microstructure development in steels. Second, it has been demonstrated that kinetic transitions are possible. Indeed, several authors have presented evidence of a transition from PE kinetics at short times (high velocity) to LE-NP kinetics at long times (low velocity).[8–10] Since in many cases (especially those involving austenite-stabilizing elements like Ni and Mn) the PE and LE-NP limits are quite separate, and diagrams of the kind in Figure 1 are accessible to computation, they are useful aids in the design of critical experiments which could ultimately be used to develop and validate improved models of ferrite growth.

One of the first models to predict a kinetic transition from PE to LE-NP interfacial contact conditions during the course of a grain boundary precipitation reaction was due to Odqvist et al.[11] These authors described the planar growth of proeutectoid ferrite in a Fe-C-Ni alloy and showed the predicted trajectory of an interfacial "tie-line" with time, beginning with a PE tie-line (parallel to a component ray) and ending with a full equilibrium tie-line. This model assumed a semi-infinite austenite grain size and incorporated energy dissipation due the interaction of solute with the interface and the buildup of the alloying element spike as per the model of Hillert and Sundman.[12] However, when the predicted evolution of the carbon conditions at the interface were coupled with a simple model for bulk C diffusion, the resulting ferrite growth kinetics were still much faster than those observed experimentally.

A second approach to the same problem was developed by Hutchinson et al.[8] who used a discrete model for the atomic jumps at the interface instead of the continuum treatment used by Odqvist et al.[11] The model of Hutchinson et al.[8] considered that a steady net flux of Ni across the interface would lead to the eventual buildup of a "spike" in the austenite and a consequent transition from initial PE to LE-NP conditions. This treatment worked well for the Fe-Ni-C system in spite of the fact that the dissipation associated

with the flux of the substitutional element was not considered. This limitation precluded the application of the model to systems where a significant dissipation (solute drag effect) is expected.

Other recent approaches to the modeling of the transition problem are due to Guo and Enomoto,[13] who included a solute drag term in their treatment of ferrite growth in Fe-C-Mn-Si alloys, and Viardin et al.,[14] who used a phase-field approach to predict a transition from PE with time.

Some recent experimental studies are relevant here. The controlled decarburization technique was used to study the kinetics of ferrite layer growth into three component austenites containing carbon and Ni,[15,16] Mn,[17,18] and Mo[16,19]. More traditional precipitation data on the Ni and Mn containing systems were obtained by Oi et al.[9] and Hutchinson.[8] Guo et al.[10] employed high-resolution microanalysis to demonstrate the existence of Mn enrichment at quenched ferrite-austenite interfaces after isothermal transformation for as little as 600 s. at 1023 K (750 °C) and well-developed Mn profiles in both ferrite and austenite after cessation of fast ferrite growth. Chen and van der Zwaag[20,21] used an elegant thermal cycling method to demonstrate the presence of "buried Mn spikes," planted in austenite by previous thermal cycles, via their kinetic interaction with moving transformation interfaces. Their in situ dilatometric studies were carried out at rather higher temperatures [>1123 K (850 °C)].

It is clear that further advances in modeling are required to account, quantitatively and self-consistently, for the following:

- Solute drag (here interpreted as trans-interfacial diffusional dissipation);
- Austenite grain size effects;
- Near cessation of ferrite growth at non-equilibrium fractions ("stasis"); and
- The relaxation times for transitions from initial PE contact conditions.

Some of these challenges are addressed in the present contribution.

II. SELF-CONSISTENT MODEL FOR FERRITE GROWTH

A. Key Physical Processes

In order to model the kinetics of ferrite growth, it is necessary to develop a description for the following processes:

- Alloying element diffusion across the interface and the dissipation associated with it.
- Evolution of the corresponding carbon concentrations at the interface.
- Carbon diffusion in the bulk phases.
- Ferrite growth as dictated by the carbon mass balance at the interface.

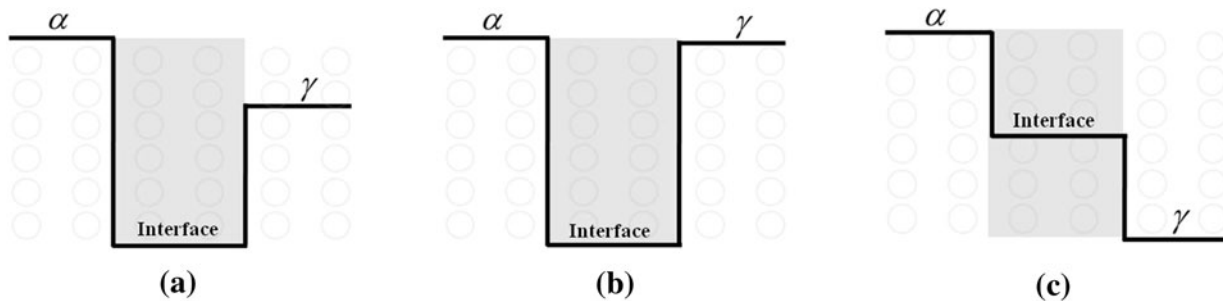Each of these processes is described in detail in the following sections:

Fig. 2—Schematic of X chemical potential profiles across the interface: (a) general case, (b) Fe-Mo, (c) Fe-Ni.

1. Alloying element diffusion

It is generally assumed that initial ferrite growth occurs under PE conditions due to the high initial interface velocity. The PE condition is not a long-lived state because a chemical potential difference for the substitutional solutes will generally be present across the interface and this will drive the diffusion of the alloying element across the interface and change the interfacial conditions. In addition to diffusional jumps that are driven by the chemical potential difference between ferrite and austenite, it is also possible to have diffusion within the interface due to the presence of a potential well which is associated with the interaction of the alloying element with the interface. Figure 2(a) shows the most general case, in which there is a difference between the chemical potentials of the substitutional element in ferrite and austenite as well as a potential well at the interface.

Two limiting cases are worth emphasizing; in the Fe-Mo-C system, it is possible to choose combinations of temperature and composition which will lead to the same chemical potential of Mo in ferrite and austenite. The interaction of Mo with the interface leads to a potential well as shown in Figure 2(b). This profile resembles the potential well often used for modeling interfacial dissipation during grain growth or recrystallization. The other extreme is that shown in Figure 2(c), where the interaction of the alloying element with the interface is weak and the dominant driving force for diffusion of the alloying element is the difference between the chemical potentials of ferrite and austenite. This is exemplified by the Fe-Ni-C and Fe-Mn-C systems.

Most treatments of diffusion within the interface are continuum treatments[22–25] that predict sharp concentration gradients within the interface. We have adopted a discrete-jump model for diffusion across the interface (in the spirit of Hutchinson et al.[8]) because the existence of concentration gradients over distances of the order of the atomic spacing is questionable. The model is similar to that of Lucke and Stuwe;[25] the interface is assumed to consist of two atomic layers, as shown in Figure 3, and diffusion from one side of the interface to the other involves 3 jumps—one jump from ferrite into the interface, another jump within the interface, and finally a jump from the interface to austenite (It should be noted that the "square" chemical potential profiles in Figure 2 are intended to schematically show the relative levels at
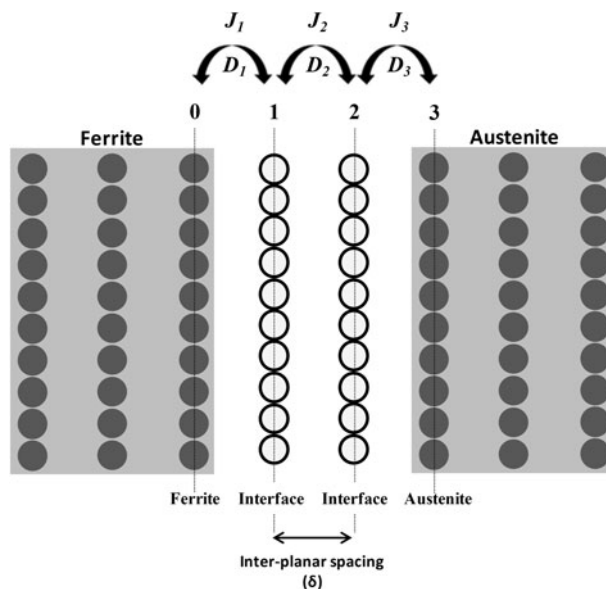

Fig. 3—Interface model in terms of atomic planes (0,1,2,3) and definition of the various diffusivities (D_1, D_2, D_3), jumps, and fluxes (J_1, J_2, J_3).

the different atomic planes, and are not to be interpreted as continuum).

The jumps in Figure 3 are assumed to occur with diffusion coefficients of D_1, D_2, and D_3. The evolution of the alloying element mole fraction on plane "i," dx_X^i as a result of these jumps can be expressed as

$$dx_X^i \cdot \frac{\delta}{V_m dt} = J_X^i - J_X^{i+1} + \frac{v}{V_m}\left(x_X^{i+1} - x_X^i\right) \quad [3]$$

where the flux term from plane "$i-1$" to plane "i," J_X^i is given by

$$J_X^i = -\frac{D_X^i}{V_m RT} x_{Fe}^{i-1} x_X^{i-1} \cdot \frac{\left(\mu_X^i - \mu_X^{i-1}\right) - \left(\mu_{Fe}^i - \mu_{Fe}^{i-1}\right)}{\delta} \quad [4]$$

In this equation, D_X^i are the diffusion coefficients of the substitutional element (X) as defined in Figure 3, R is the gas constant, dt is the time increment used in the calculations, δ is the distance between atomic planes, and v is the interface velocity.

The interface velocity will evolve during ferrite growth leading to non-steady-state conditions. However, for a sufficiently small time increment, dt, it is reasonable to assume steady-state and the left hand side of Eq. [3] tends

to zero. As a result, for a given interface velocity, and assuming that the transformation is non-partitioning, i.e., X_X^0 = constant, one can calculate the concentration of X at each atomic plane. The dissipation associated with diffusion across the interface (solute drag) can then be calculated using a discrete-jump version of the expression proposed by Hillert and Sundman[12]:

$$\Delta G^{\text{dissipated}} = -\frac{V_m}{v} \int_{-\delta}^{+\delta} J_M \cdot \frac{d(\mu_M - \mu_{Fe})}{dy} \cdot dy \quad [5]$$

$$\Delta G^{\text{dissipated}} = \sum_{i=1}^{i=3} -\frac{V_m}{v} \cdot J_X^i \cdot \left[\left(\mu_X^i - \mu_X^{i-1} \right) - \left(\mu_{Fe}^i - \mu_{Fe}^{i-1} \right) \right] \quad [6]$$

The concentration of the alloying element across the interface and the associated dissipation can thus be expressed as a function of velocity. The associated carbon concentrations can then be calculated using the procedure described in Section II–A–2.

2. Evolution of carbon concentrations at the interface

Given the high diffusivity of carbon, it is reasonable to assume that the carbon chemical potential is constant across the interface. In order to determine the value of the carbon chemical potential, we employ a simple energy balance across the interface:

$$\Delta G^{\text{chem}} + \Delta G^{\text{intrinsic}} + \Delta G^{\text{dissipated}} = 0 \quad [7]$$

where ΔG^{chem} is the chemical driving force given by [8]

$$\Delta G^{\text{chem}} = \frac{\left(U_X^{\text{fcc}} + U_X^{\text{bcc}} \right)}{2} \cdot \left(\mu_X^{\text{fcc}} - \mu_X^{\text{bcc}} \right) + \frac{\left(U_{Fe}^{\text{fcc}} + U_{Fe}^{\text{bcc}} \right)}{2} \cdot \left(\mu_{Fe}^{\text{fcc}} - \mu_{Fe}^{\text{bcc}} \right) \quad [8]$$

where U_X and U_{Fe} are the mole fraction of "X" and "Fe," respectively, on the substitutional lattices in the alloy (U-fraction).

As expected, the driving force expressed by Eq. [8] is zero for the limiting cases of PE and LE-NP. Under most conditions of interest in the present work, the intrinsic dissipation term (due to the structural rearrangement at the interface) is negligible and Eq. [7] reduces to

$$\Delta G^{\text{chem}} + \Delta G^{\text{dissipated}} = 0 \quad [9]$$

This equation along with the assumption of constant carbon chemical potential is sufficient to determine the carbon concentrations on the ferrite and austenite sides of the interface as well as the carbon concentrations within the interface. When this calculation is performed as a function of velocity, it is possible to trace, on the ternary isotherm, the interfacial compositions that the system will sample as it evolves from PE to LENP. Two examples are shown in Figure 4. The first is for Fe-Ni-C at 1048 K (775 °C) (Figure 4(a)) and the second is for Fe-Mo-C (Figure 4(b)) at the same temperature. In this calculation, the diffusion coefficients for the various jumps within the interface were assumed to be equal to the bulk diffusion coefficient in ferrite for the first jump, D_1, equal to the bulk diffusion coefficient in austenite for the third jump, D_3, and equal to the geometric average of D_1 and D_3 for the second jump, D_2.

It is clear from Figure 4 that the path from PE to LENP can be complicated due to the effect of dissipation on the interfacial carbon concentration. This point is important for understanding the evolution of the system and the overall growth kinetics and will be discussed in detail in Section IV.

3. Carbon diffusion in the bulk phases

Sections II–A–1 and II–A–2 described the evolution of interfacial conditions as a function of velocity. In order to derive the actual kinetics as a function of time, it is necessary to incorporate carbon diffusion in the
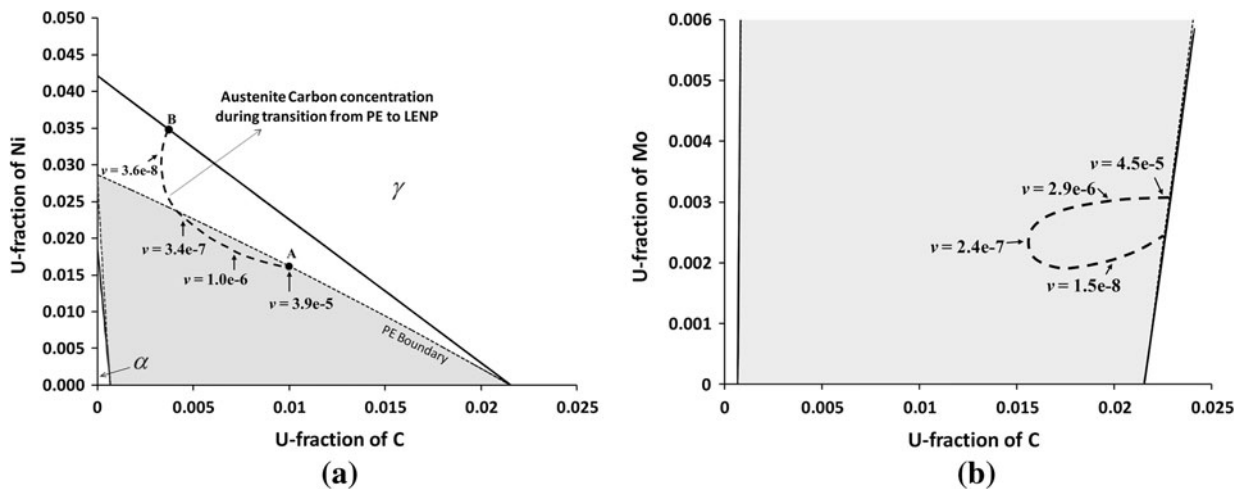

Fig. 4—Isothermal sections for (a) Fe–Ni-C and (b) Fe-Mo-C at 1048 K (775 °C), plotted as U_X vs U_C. Path taken by the system is shown along with arrows indicating interface velocity (v) in units of m/s.
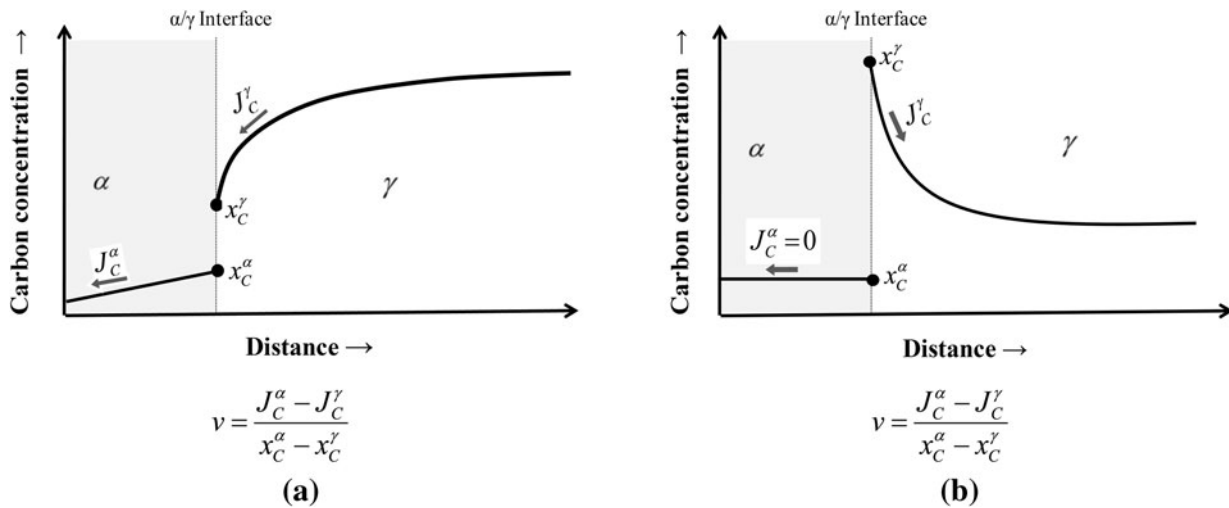
Fig. 5—Schematics of C profiles in (*a*) decarburization and (*b*) precipitation, along with velocity equations for the two different cases.

bulk phases. Two cases are considered in this contribution; ferrite precipitation at austenite grain boundaries and ferrite growth during controlled surface decarburization treatments.[15–19,26–28] The first situation is the case that is of industrial relevance for microstructure evolution in steels, which has been studied for more than 50 years. Here, it is sufficient to model only carbon diffusion in the austenite phase. The case of decarburization, which offers some advantages in terms of precision of growth kinetic data,[15–19,26–28] requires the calculation of the carbon profiles in both austenite and ferrite. In both cases, carbon diffusion is modeled using a Murry-Landis explicit finite-difference method that includes the carbon dependence of the carbon diffusivity in austenite. In the case of decarburization, the specimens are large enough that they can be assumed to be semi-infinite, and overlap of the carbon diffusion profiles in the austenite does not take place (Figure 5(a)). In contrast, the overlap of the carbon diffusion profiles in the austenite is critical for capturing the kinetics of ferrite precipitation (Figure 5(b)).

In order to capture the kinetics accurately in the case of ferrite precipitation, and to estimate the ferrite volume fraction, a spherical geometry was assumed and the diameter of the sphere was set equal to the experimentally determined grain size.

4. Growth rate

The instantaneous growth rate of the ferrite layer can be calculated from the mass balance at the interface. In the case of ferrite precipitation, the mass balance leads to

$$v = -\frac{J_C^\gamma}{x_C^\alpha - x_C^\gamma} \qquad [10]$$

For decarburization, calculation of the interface velocity requires consideration of the carbon flux in both ferrite and austenite. The velocity is then given by the expression

$$v = \frac{J_C^\alpha - J_C^\gamma}{x_C^\alpha - x_C^\gamma} \qquad [11]$$

B. *Model Parameters*

In order to implement the above model, it is essential to have reliable thermodynamic and kinetic data. The thermodynamic description of the bulk ferrite and austenite phases in the Fe-Ni-C and Fe-Mo-C systems was obtained from the TCFE2 database which was accessed using the TQ interface of the ThermoCalc Software Package.[29] In the case of the Fe-Mn-C system, the TCFE2 description appears to systematically underestimate the solubility of Mn in ferrite. For this reason, we have developed a modified description which is described in the Appendix. As for the kinetic data, the bulk diffusion coefficients of the substitutional elements were extracted from the Mob2 database, which is also available from ThermoCalc. The carbon diffusion coefficient in austenite was obtained from Reference 30, while the carbon diffusion coefficient in ferrite was measured experimentally from decarburization experiments on binary Fe-C alloys.[31]

A key challenge is to develop a thermodynamic description of the interface and to estimate the diffusion coefficients for transport across the interface. We have employed the approach of defining an interface-phase as proposed by Hillert.[32] For simplicity, the Gibbs energy expression of this phase was developed by modifying that of the bulk austenite phase in the following manner:

1. The reference state for the free energy was shifted by 3.5 kJ/mol in order to capture an interfacial energy of the order of 0.5 J/m^2.
2. The Fe-X interaction term in the substitutional sublattice was decreased in order to favor the segregation of the alloying element to the interface or increased in order to favor desegregation. While accurate values of the interaction parameter are not available, reasonable estimates could be made based on the measured binding energies of alloying elements to grain boundaries.

In the literature, many different values for the cross-interface diffusivities have been used and these vary over many orders of magnitude.[13,33–37] For this reason, the

three diffusion coefficients D_1, D_2, and D_3 were initially used as adjustable parameters. However, it quickly became apparent that in order to capture the experimental trends, it was necessary to use values of the cross-interface diffusion coefficient that are of the same order of magnitude as those in the bulk phases. This is consistent with the conclusions of recent applications of solute drag theory to recrystallization.[33] Therefore, all of the results presented in subsequent sections were obtained using the bulk ferrite diffusion coefficient for D_1, the bulk austenite diffusion coefficient for D_3, and the geometric average of the two for D_2. In addition to providing an excellent description of the experimental data, the present approach effectively removes three adjustable parameters from the model. From the mechanistic point of view, the use of these values is attractive because one would expect that jumps to and from ferrite would be dominated by attachment kinetics in ferrite and thus would have a similar diffusion coefficient as bulk diffusion in ferrite. Similarly, jumps to and from austenite would occur at a similar rate to jumps within the bulk austenite. It is worth pointing out that atomistic simulations seem to confirm that diffusion across the interface occurs at a rate comparable to bulk diffusion.[38,39]

Based on the above discussion, the only fitting parameter in the model is the interaction parameter of Fe and X within the interface. As will be shown in Section III, excellent agreement with the experimental data is obtained by estimating this parameter from grain boundary binding energies.

III. APPLICATION OF THE MODEL

The evolution of contact conditions during growth is dominated by the alloying element diffusion within, and across, the interface. Two extremes can be identified:

a) A situation where the interaction of the alloying element with the interface itself is weak (*i.e.*, the binding energy of the solute to the boundary is small compared to the chemical potential difference between ferrite and austenite). This case is exemplified by the Fe-Ni-C and Fe-Mn-C systems.

b) The second extreme is exemplified by Mo at temperatures in the range of 1048 K to 1123 K (775 °C to 850 °C). In this temperature range, the chemical potentials of Mo in ferrite and austenite are almost identical. The dominant effect is due to Mo interaction with the interface, much like the interaction of solutes with grain boundaries.

These three systems are discussed in detail in the following Sections. However, it should be emphasized that the model is not limited to these systems and that it can be applied to the most general case in which both types of interactions are important and this is illustrated in the companion paper in this volume.[40]

A. *Fe-C-Ni and Fe-C-Mn*

In order to validate the model, it is necessary to identify discriminating experimental data that provide a critical test of the model. The key weakness of ferrite precipitation data is that there is large scatter in the reported allotrimorph half-widths due to nucleation, crystallography, stereology, and variations in the grain size. For this reason, we have avoided direct comparison of the measured and predicted allotrimorph width. Instead, we have focused on the measured ferrite volume fraction at long holding times and the critical compositions and temperatures for partitionless ferrite growth. We have therefore modeled the results of Oi *et al.*[9] in which the critical temperature for the cessation of ferrite growth was measured (Figures 6(a) and (c)) and the data of Hutchinson *et al.*[8] for which the critical composition for ferrite growth stasis at 973 K (700 °C) was measured (Figure 6(b)).

The best fit of the effective cessation of ferrite growth was obtained by adjusting the interaction parameter between Fe and Ni in the interface such that the initial chemical potential of Ni in the interface is 1.5 kJ/mol greater than the average of the initial chemical potentials of Ni in ferrite and austenite. The choice of this value is based on the weak interaction of Ni with the interface along with the tendency for C to repel Ni from the interface. As shown in Table I, the model accurately predicts the temperature at which ferrite growth stops for the Fe-2.66pctNi-0.196pctC and 2.42pctNi-0.293pctC alloys employed by Oi *et al.*[9] Similarly, the model predicts that the volume fraction of ferrite formed at 973 K (700 °C) will dramatically decrease between 2.76pctNi and 3.14pctNi in agreement with the experimental data of Hutchinson *et al.*[8]

Similarly, in the case of the Fe-Mn-C system, the experimental trends could be captured by setting the initial chemical potential of Mn in the interface to a value which is 2.5 kJ/mol lower than the average of initial chemical potentials of ferrite and austenite. Once again, the model accurately captures the critical temperatures for the arrest of ferrite growth as shown in Table I. It should be pointed out that the quantitative agreement between the measured and calculated volume fractions can be improved by varying the values of the diffusion coefficients and binding energies for each alloy and temperature. However, we prefer to maintain constant values of these parameters in order to focus on the physical picture. In addition, one should not expect perfect agreement given the inherent simplifications in the model as well as the uncertainties associated with cross-interface diffusivities, binding energies and bulk carbon diffusion coefficients.

In order to obtain a greater insight into the mechanisms responsible for the cessation of ferrite growth, the interfacial carbon concentration on the austenite side of the interface and the carbon flux in austenite are plotted in Figure 7, as a function of time for two cases, Fe-2.41pctNi-0.078pctC and Fe-2.08pctMn-0.095pctC, both at 973 K (700 °C). For the sake of clarity, Figure 7 was constructed for a grain size of 500 μm in order to postpone the overlap of the carbon diffusion profiles in austenite. Both compositions lie inside the envelope of no partition. In both cases, the interface stops because the carbon concentration at the interface drops below the carbon concentration ahead of the interface. The
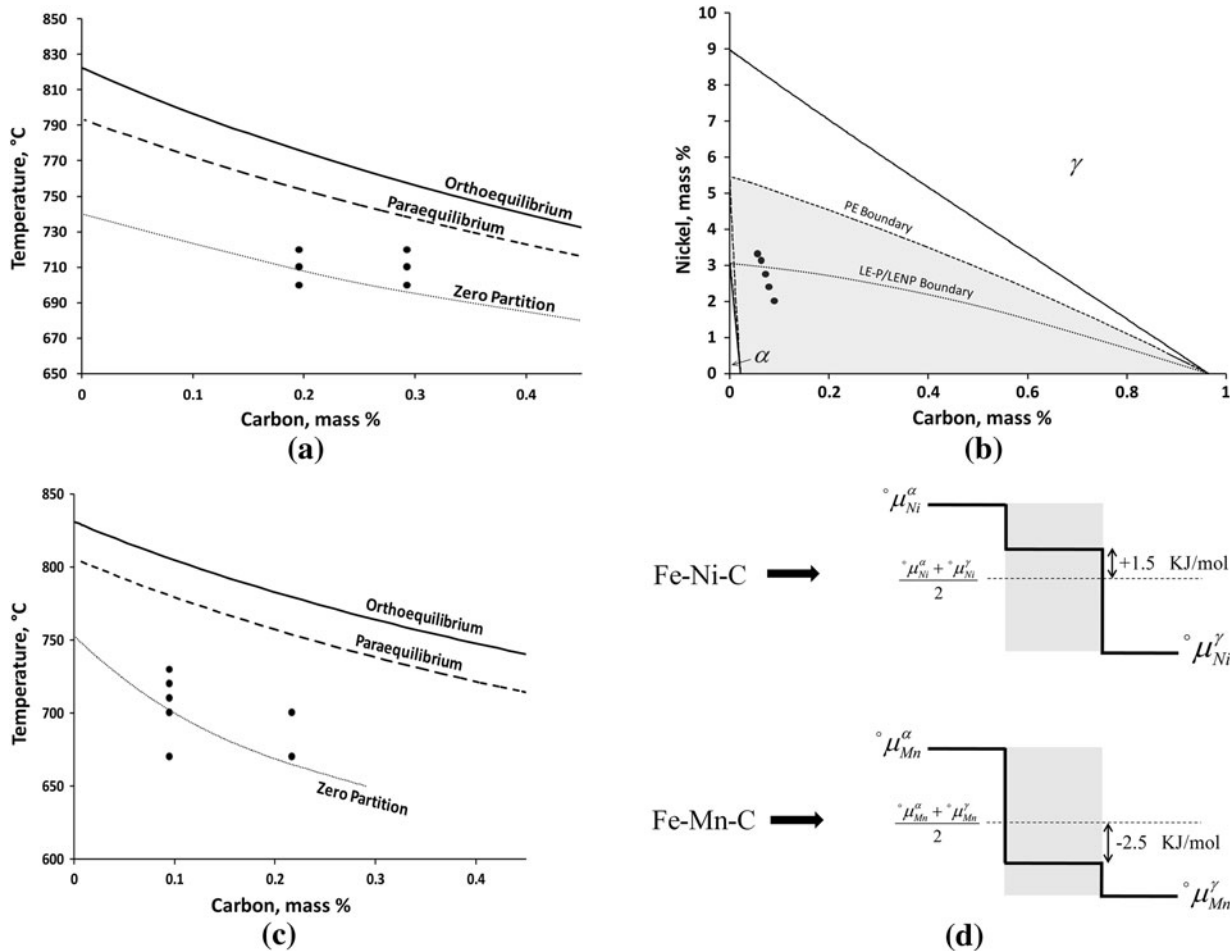
Fig. 6—(a) 2.5 wt pct Ni isopleth with experimental conditions (black circles) examined by Oi *et al.*,[9] (*b*) Isothermal section of Fe-Ni-C phase diagram at 973 K (700 °C) with five alloy compositions examined by Hutchinson *et al.*,[8] (*c*) 2.0 wt pct Mn isopleths with different experimental conditions examined by Oi *et al.*,[9] (*d*) Schematic of the initial chemical potential profiles used for calculations in Fe-Ni-C and Fe-Mn-C systems.

Table I. Experimentally Obtained Ferrite Volume Fraction and New Model Predictions for Different Fe-Ni-C and Fe-Mn-C Alloys at Different Temperatures

| Alloy	Temperature K (°C)	Measured (V_f)	Calculated (V_f)
2.66pctNi-0.196pctC	973 (700)	47 pct	34 pct
	983 (710)	n/a	20 pct
	992 (720)	3 pct	0 pct
2.42pctNi-0.293pctC	973 (700)	21 pct	18 pct
	983 (710)	<1 pct	0 pct
	993 (720)	0 pct	0 pct
2.02pctNi-0.088pctC	973 (700)	82 pct	81 pct
2.41pctNi-0.078pctC		77 pct	79 pct
2.76pctNi-0.071pctC		66 pct	76 pct
3.14pctNi-0.062pctC		<10 pct	26 pct
3.33pctNi-0.055pctC		<10 pct	22 pct
2.08pctMn-0.095pctC	943 (670)	67 pct	35 pct
	973 (700)	23 pct	32 pct
	983 (710)	3 pct	4 pct
	993 (720)	n/a	0 pct
	1003 (730)	0 pct	0 pct
2.17pctMn-0.217pctC	943 (670)	18 pct	6 pct
	973 (700)	0 pct	0 pct
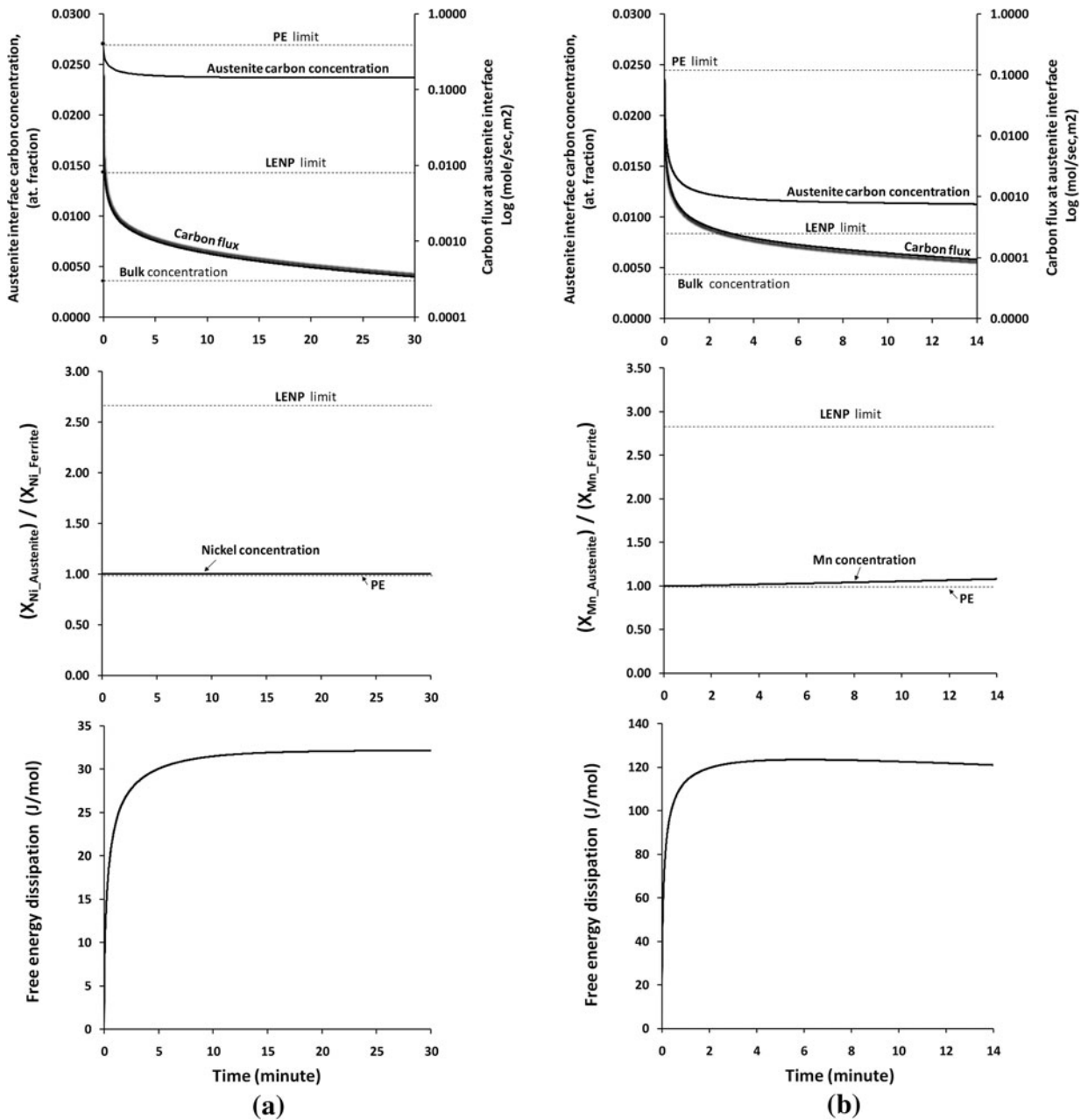
Fig. 7—Evolution of carbon concentration, carbon flux, and substitutional alloying element concentration on the austenite side of the interface as a function of time in (a) 3.14pct Ni-0.062pct C alloy, (b) Fe-2.08pctMn-0.095pctC alloy. The free energy dissipation for each alloy as function of time is also presented in the last row.

drop in carbon concentration at the interface is a result of the buildup of the alloying element spike in austenite as well as the dissipation of energy which requires an increase in the supersaturation for growth to continue. The relative contributions of these two effects will be the subject of further analysis in Section IV–A.

In both of the above cases, the bulk composition was within the envelope of no partitioning, therefore the interface could, in principle, continue moving forward once the carbon diffusion profile in austenite has sufficiently relaxed. In such a case, ferrite growth will resume and the volume fraction would increase beyond the predicted values shown in Table I. This resumption

of growth may in fact be responsible for the discrepancy between the calculated and measured volume fractions just below the LENP limit [e.g., 29 vs 47 pct for the 2.76pctNi alloy at 973 K (700 °C)]. On the other hand, in an alloy the bulk composition of which is outside the envelope, one would expect the interface to stop and further growth to occur very slowly under full-partitioning conditions.

As mentioned earlier, a limitation of ferrite precipitation data is that the reported measurements show a large scatter and this is not ideal for critical tests of ferrite growth models. An alternative is to use the kinetics of ferrite growth under decarburization
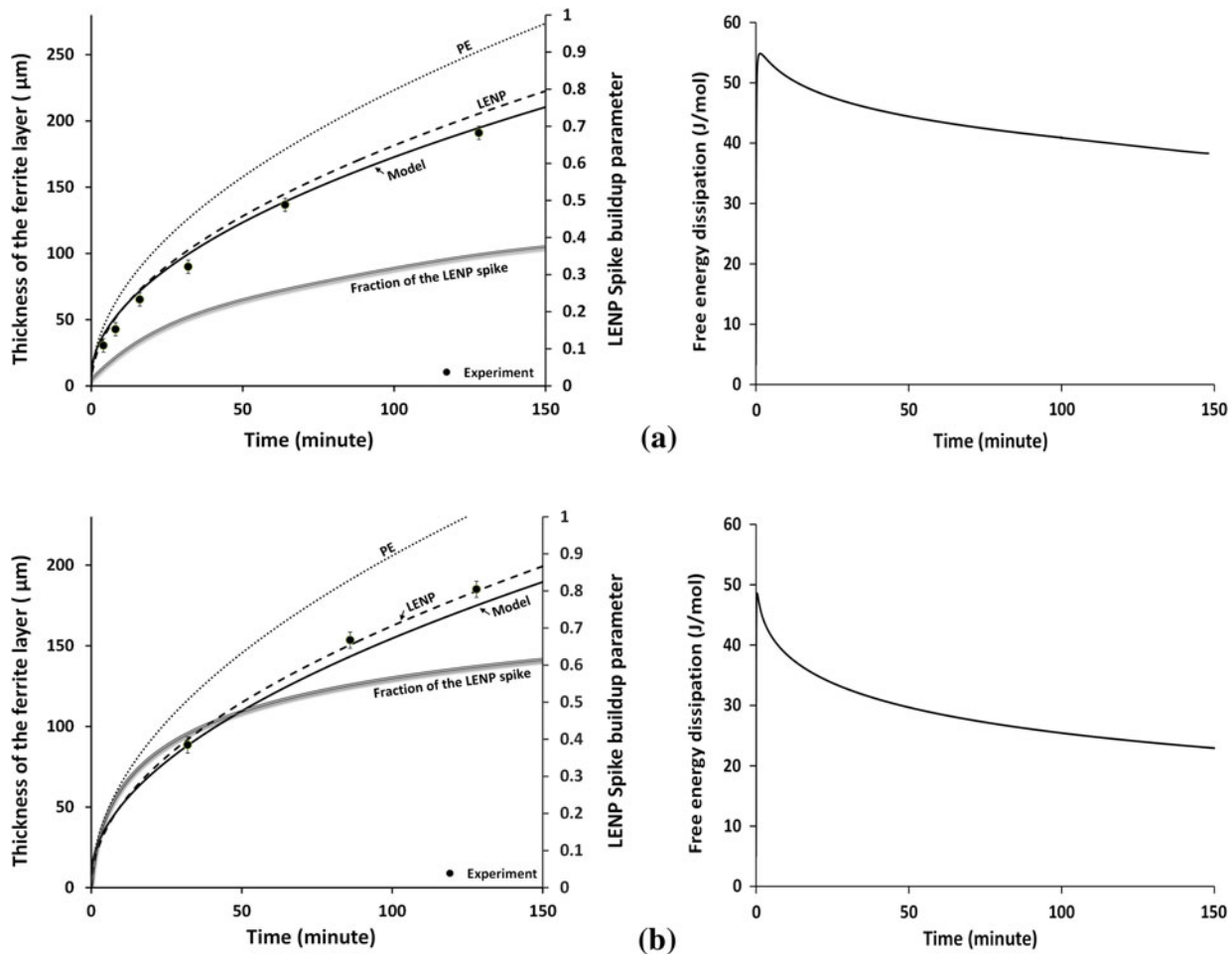
Fig. 8—Kinetics of decarburization (left) and evolution of free energy dissipation (right) in Fe-0.94pctMn-0.57pctC alloy at (*a*) 1028 K (755 °C), (*b*) 1048 K (775 °C); the secondary axis in the left column is presenting the LENP spike buildup parameter (P_{Spike}) which is defined in the text and varies from 0 in the case of PE to 1 in the case of LENP.

conditions where the kinetics can be measured with high precision.[15–19,26–28] The kinetics of decarburization in the Fe-Mn-C system were examined in detail for a range of Mn contents (0.5 to 2 pctMn) and temperatures [998 K to 1147 K (725 °C to 874 °C)].[17,19] Using the same cross-interface diffusion coefficients and interface binding energies described above for ferrite precipitation, the model shows excellent agreement with the experimental kinetics measurements as shown for selected conditions in Figures 8 and 9. In order to aid subsequent discussions, Figures 8 and 9 also include the energy dissipation and height of the alloying element spike for each of the conditions considered.

B. Fe-C-Mo

The Fe-Mo-C system offers an excellent opportunity to test models that include the effects of energy dissipation due to cross-interface diffusion. The reason is that compositions and temperatures can be chosen where the chemical potentials of Mo in the ferrite and austenite of bulk composition are the same. As a result, there is no spike and the consequential changes in

contact conditions can be ignored. The dominant interaction is that of Mo with the potential well at the interface. In order to test the model, we have examined the kinetics of ferrite growth under decarburization conditions in Fe-0.51pctMo-0.54pctC alloy. The cross-interface diffusion coefficients D_1, D_2, and D_3 were assumed to be equal to the ferrite, geometric average, and austenite diffusion coefficients, respectively. The interaction coefficient of Fe and Mo in the interface was varied such that the initial chemical potential of Mo in the interface is 15 kJ/mol lower than the average initial chemical potentials of ferrite and austenite. The results of the calculations are compared with experimental measurements in Figure 10 for temperatures of 1048 K, 1079 K, and 1098 K (806 °C, 775 °C, and 825 °C). The agreement is excellent in all cases. It is particularly interesting to point out that the experimental kinetics appeared to be parabolic, which suggests that the interfacial conditions were not changing. In the past,[16] this led us to conclude that the energy dissipation was constant, which is inconsistent with solute drag theories where a velocity dependence is expected. However, calculations using the new model suggest, as shown in
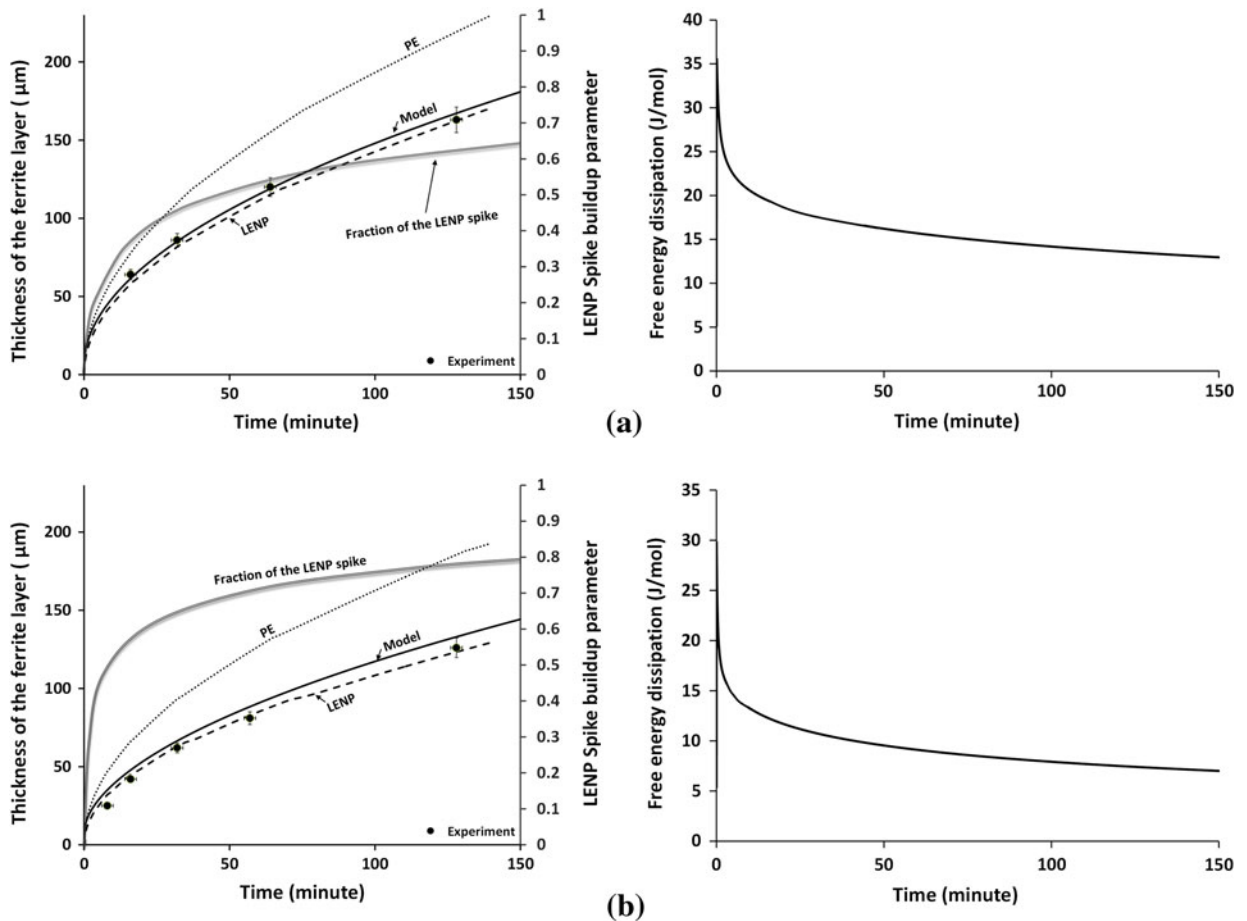
Fig. 9—Kinetics of decarburization (left) and evolution of free energy dissipation (right) in Fe-0.94pctMn-0.57pctC alloy at (*a*) 1079 K (806 °C), (*b*) 1098 K (825 °C); the secondary axis in the left column is presenting the LENP spike buildup parameter (P_{Spike}) which is defined in the text and varies from 0 in the case of PE to 1 in the case of LENP.

Figure 10, that the dissipation is decreasing only slowly with time and this gives kinetics that are close to parabolic over the times investigated here.

IV. DISCUSSION

A. *Key Features of the Model*

A model for planar ferrite growth in Fe-C-X systems has been presented in Section II. The model self-consistently incorporates alloying element diffusion across the interface and the dissipation associated with it, the evolution of the corresponding carbon concentrations at the interface, the carbon diffusion in the bulk phases, and the ferrite growth rate. The model may be viewed as a hybrid of the earlier approaches presented by Odqvist *et al.*[11] and Hutchinson *et al.*[8] The model considers a discrete-jump approach at the interface in the spirit of the models of Hutchinson *et al.*[8] and Lucke and Stuwe[25] and it incorporates dissipation using the approach of Odqvist *et al.*[11] The model differs from the earlier approach presented by Hutchinson *et al.*[8] in two important ways; the first is that dissipation due to solute diffusion in the interface is taken into account and the

second is that convection is described in terms of Eq. [3] as opposed to the probability term used earlier.[8] The key differences in comparison to the model of Odqvist *et al.*[11] are the discrete nature of the jumps, the smaller cross-boundary diffusion coefficients, the finite grain size, and the consideration of the driving force and dissipation over the interface only. Table II, provides a summary of the parameters used in the present model compared to earlier ones for the case of precipitation in Fe-Ni-C at 973 K (700 °C). While the predictions of the present model are similar to those of Hutchinson *et al.*[8] for the case of the Fe-Ni-C system, a key difference is the size of the Ni spike in austenite. In the treatment of Hutchinson *et al.*,[8] the temporary cessation of ferrite growth for some alloys lying within the no-partitioning envelope (*e.g.*, alloy containing 2.76 wt pct Ni) was due to the rapid kinetics of Ni spike development and the subsequent lowering of the carbon contact condition in the austenite below that in front of the interface. In the present model, both dissipation and spike buildup contribute to the drop of the carbon concentration at the austenite side of the interface which leads to the cessation of ferrite growth. As a result, a much smaller spike is predicted prior to the cessation of ferrite growth
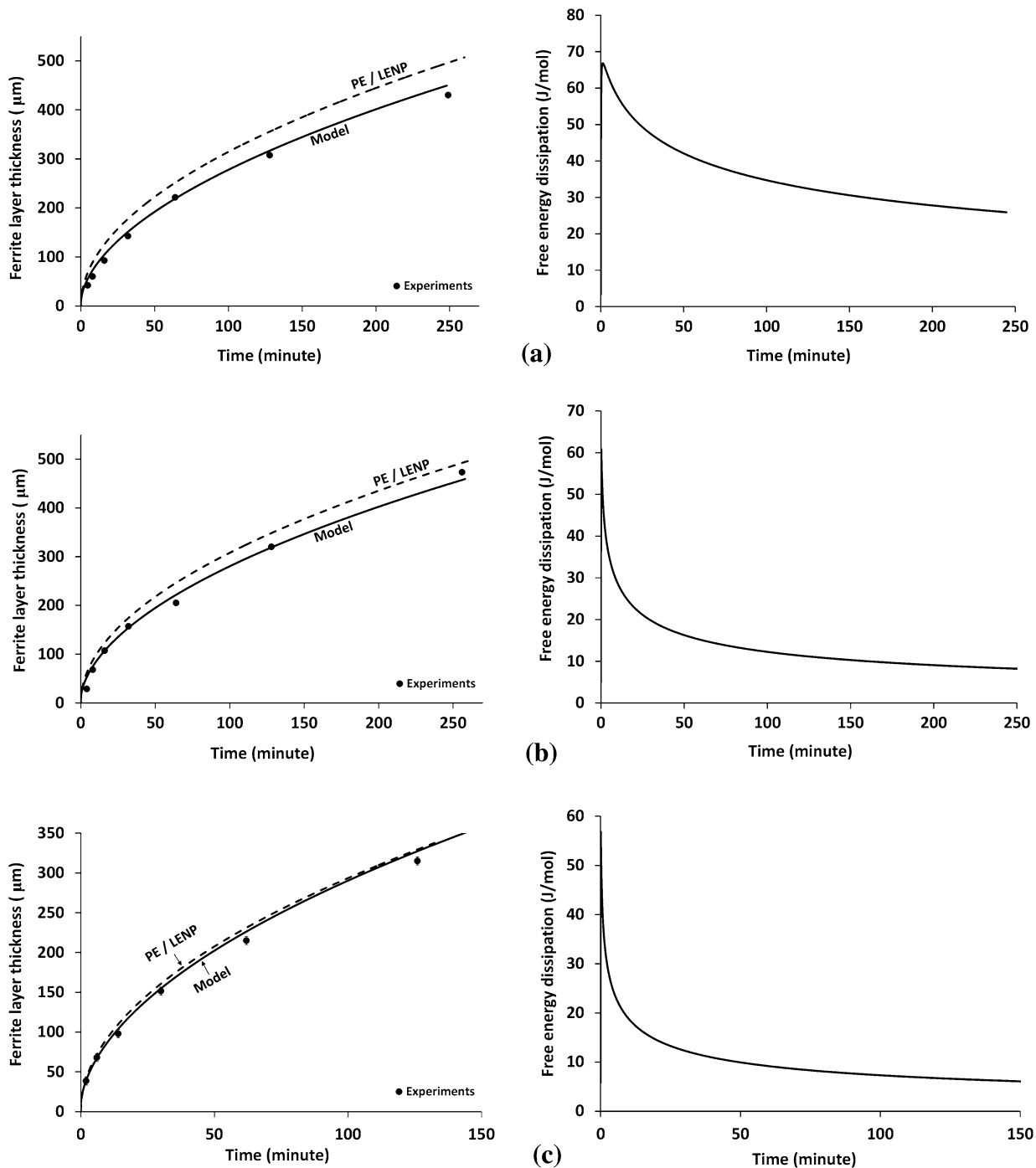
Fig. 10—Kinetics of decarburization and evolution of free energy dissipation in Fe-0.51pctMo-0.54pctC alloy at (a) 1048 K (775 °C), (b) 1079 K (806 °C), (c) 1098 K (825 °C).

in the present model compared to that of Hutchinson et al.[8] This point is illustrated in Figure 7(a), which shows an example in which the cessation of ferrite growth occurred without an appreciable buildup of the Ni spike in austenite. The dominant contributor to the stoppage of ferrite growth in this case is energy dissipation (solute drag). Interestingly, similar calculations for an alloy with 2.08 pct Mn-0.095 pct C at the same temperature, Figure 7(b), suggest an important

role of spike buildup. It can be seen in Figure 7(b) that energy dissipation has already peaked prior to the cessation of ferrite growth, which suggests that the change of carbon concentration due to dissipation is not responsible for the stoppage. On the other hand, the height of the spike continued to build up and in this case, it led to the arrest of ferrite growth. The difference between the two alloys is probably due to the fact that the diffusion coefficient of Mn is nearly 40 times that of

Table II. Summary of the Parameters Used in the Present Model Compared to Earlier Models by Odqvist et al.[11] and Hutchinson et al.[8] for the Case of Precipitation in Fe-Ni-C at 973 K (700 °C)

	Hutchinson et al.[8]	Odqvist et al.[11]	Present Model
Driving Force	across the interface	for the whole system	across the interface
Dissipation	not included	for the whole system	for the interface only
Diffusion Coefficients Within Interface	Sqrt$(D_\alpha \times D_\gamma)$	7.4E−13 m^2/s	three jumps with coefficients of: D_α, Sqrt$(D_\alpha \times D_\gamma)$ and D_γ
Diffusion Model Within Interface	discrete transient	continuum steady-state	discrete steady-state
Interface Thermodynamics	n/a	liquid mixing model, with FCC interaction parameters $\Delta L \sim 2.5RT$	modified description of FCC $\Delta L \sim +1.5$ kJ/mol

Ni, which aids the development of the spike in the Mn alloy. An important consequence of this comparison is that the relative contributions of spike buildup and energy dissipation to the cessation of ferrite growth are very sensitive to the choice of diffusivities. The general trend, however, is that the combined effect of these two processes results in the arrest of ferrite growth.

The predictions of the present model also differ from those of Odqvist et al.[11] because of the differences in binding energies and diffusivities used. In addition, the Odqvist model was applied to precipitation in semi-infinite specimens compared to the application to finite spherical grains in this work. This is an important difference critical in explaining the effect of grain size on transformation kinetics and is described in Section IV–C.

B. Critical Assessment of the Model

The cross-interface diffusivities have been set to values determined directly from the known diffusivities in the bulk phases and are hence not adjustable parameters. The only parameter that is adjusted is the binding energy of the solute to the interface and this has been chosen on the basis of segregation data to grain boundaries. This model has been tested on three systems: Fe-Ni-C and Fe-Mn-C, which are examples where the interaction between the alloying element and the interface is thought to be weak, but where a significant chemical potential difference for the substitutional element between the ferrite and austenite of bulk compositions exists, and Fe-Mo-C, where the interaction with the interface is large, but the chemical potential difference across the interface is negligible. These systems allow a rigorous test of two origins of energy dissipation at the interface that occur in such systems—energy dissipation due to the cross-interface diffusion necessary for spike accumulation and energy dissipation due to diffusion in the interface alone where there is a strong interaction with the interface. Two sets of experimental data were chosen for model validation—ferrite precipitation data and ferrite growth data under decarburization conditions. These choices of data for comparison are not only significant in the fact that they provide a wealth of data under different diffusion geometries, temperatures, and alloy compositions, but

also because the interface velocity ranges that are sampled in typical decarburization experiments are at least an order of magnitude slower than those in precipitation experiments. Since the dissipation due to diffusion in the interface is velocity dependent, this aspect of the data adds strength to the comparison between model and experiment. For both alloy systems and for both sets of experimental data, very good agreement between experiment and model was achieved. This indicates that the essential features of the model are probably correct.

A key test of the model was the correct prediction of the arrest of ferrite growth as a function of temperature and composition during precipitation in Fe-Ni-C and Fe-Mn-C alloys. The binding energy and cross-interface diffusivities which captured ferrite precipitation in Fe-Mn-C also provided an excellent fit of the decarburization kinetics of the Fe-Mn-C system. In particular, the model captured the close to parabolic ferrite growth kinetics under decarburization conditions. Interestingly, the experimental kinetics are occasionally very close to the predictions of the LE-NP model (e.g.,[17,19]). These observations should be interpreted with care as illustrated in Figures 8 and 9, which show the decarburization kinetics along with the parameter

$$P_{\text{Spike}} = \frac{X_{\text{Interface}} - X_{\text{PE}}}{X_{\text{LENP}} - X_{\text{PE}}}$$

where $X_{\text{Interface}}$ is the instantaneous Mn concentration at the austenite interface predicted by the model and X_{PE} and X_{LENP} are the Mn concentrations at the austenite interface under PE and LENP conditions, respectively. This parameter (P_{Spike}) varies from 0 in the case of PE to 1 in the case of LENP. It can be seen than in the case of decarburization at 1098 K (825 °C), the parameter is close to 1, meaning that the full LENP spike has developed and that the observed kinetics are indeed LENP kinetics. In contrast, at 1028 K (755 °C), only a partial spike has developed. While the experimental data are close to the LENP predictions at 1028 K (755 °C), the present model suggests that in fact there is only a partial spike, and the kinetics are due to the effect of dissipation on the interfacial conditions, i.e., LENP kinetics may be observed because there is a real spike of a magnitude close to that of the LENP model or because

the free energy dissipated due to alloying element diffusion across the interface gives rise to kinetics that look like LENP. Of course, the spectrum of combinations of spike and energy dissipation will also exist.

A second important comment needs to be made concerning the Fe-Mn-C system. In earlier works,[17,19] PE kinetics were reported at high temperatures in this system and the concept of a reduced capacity for Mn at the moving interface was introduced[17] to fit the results. Unfortunately, it is difficult to assess the above observations in the absence of a reliable thermodynamic description of the Fe-Mn-C system at the above temperatures. The presence of PE at a high temperature was based on calculations of the LENP and PE limits using the TCFE2 database. The modified thermodynamic description, in the Appendix, suggests that none of the high temperature observations reported earlier are PE. If the new database is employed, all of the earlier observations can be fitted using the present model without employing the capacity concept. We have therefore refrained from further discussing these high temperature results until a more reliable thermodynamic description is developed and agreed upon.

In the case of the Fe-Mo-C system, the apparently constant dissipation during decarburization was shown to be a natural consequence of a slowly varying dissipation with time (and interface velocity), giving a ferrite growth rate very close to parabolic.

C. Grain Size Effect in Precipitation

The role of soft impingement in precipitation and the associated effect of grain size on the ferrite volume fraction are illustrated in Figure 11, which shows the predicted evolution of an alloy containing 2.41pctNi and 0.078pctC transformed at 973 K (700 °C) for grain sizes of 10, 20, 50, 100, and 500 μm. It is clear from these simulations that the buildup of the Ni spike is very slow at this temperature and that the transition to LENP would take very long times that are unlikely to be encountered experimentally. This conclusion is similar to that reached by Odqvist et al. who modeled the transition from PE to LE-NP using a semi-infinite geometry. The role of soft impingement is critical for understanding the behavior of finite specimens because it leads to a rapid decrease in interface velocity. The
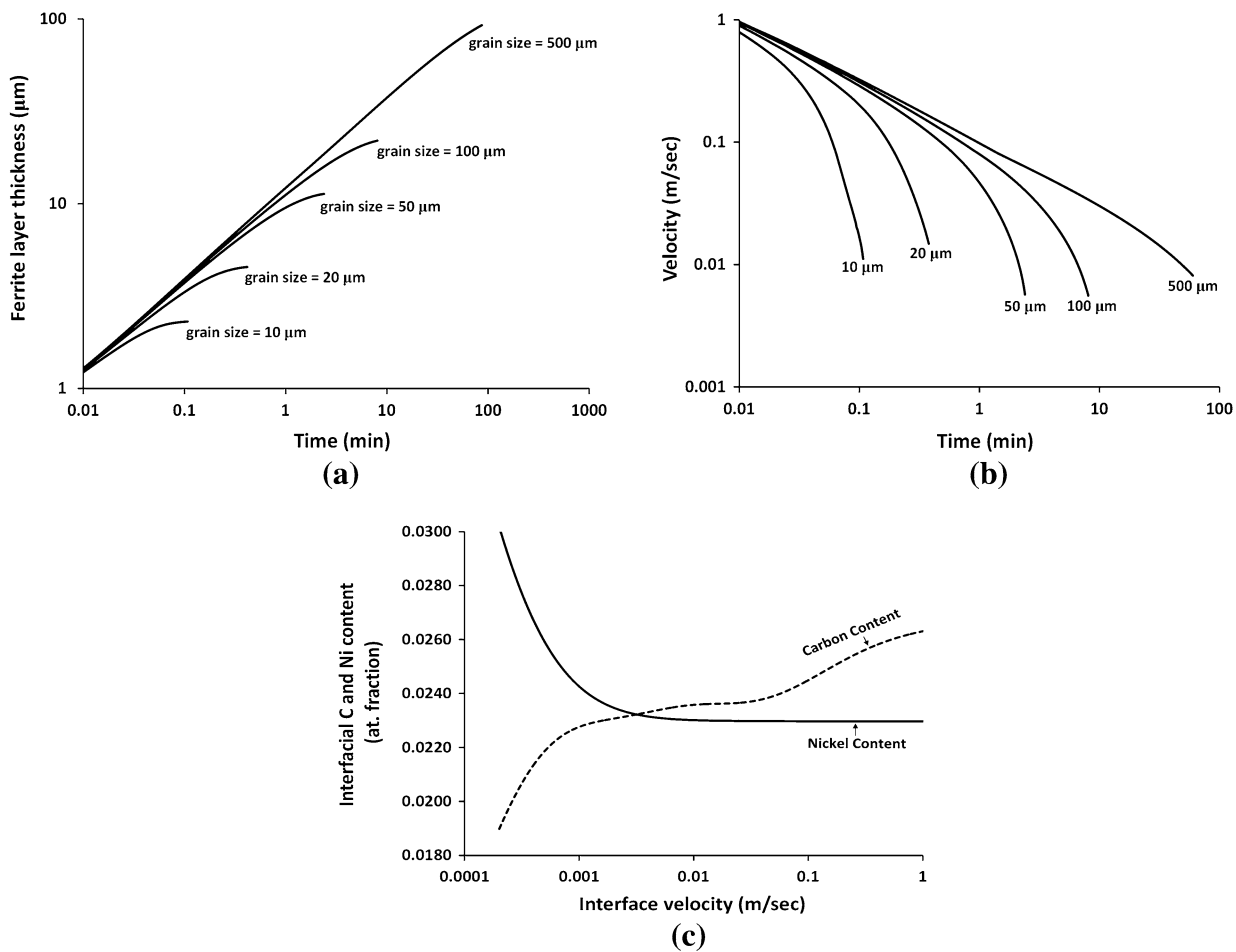

Fig. 11—Predicted evolution of ferrite layer in an alloy containing 2.41pct Ni and 0.078pct C transformed at 973 K (700 °C) for grain sizes of 10, 20, 50, 100, and 500 μm. (a) Thickness of the ferrite layer vs time, (b) Interface velocity vs time, (c) evolution of austenite nickel and carbon concentration vs. interface velocity.

drop in the Ni concentration associated with this rapid decrease in velocity finally leads to the flattening or inversion of the carbon profile in the vicinity of the interface and the arrest of ferrite growth. The predicted ferrite fractions when growth stops are 0.85, 0.84, 0.84, 0.84, 0.82, and 0.75 for samples in which the grain sizes are 5, 10, 20, 50, 100, and 500 μm, respectively. Several points are worth emphasizing at this stage:

- It is difficult to explore the evolution of the kinetics and contact conditions at low velocities using typical precipitation experiments (grain size 20 to 100 μm) because these velocities are only accessible after soft impingement. A key advantage of the decarburization method is that it permits one to easily access velocities below 1.10^{-8} m/s and estimate the operating contact conditions at these velocities. It is thus possible to observe the transition from PE to LENP experimentally under appropriate decarburization conditions. Such observations have been made and will be reported in a future contribution.

- The ferrite volume fraction appears to be independent of grain size over a wide range of conditions. Goune et al.[41] have reported experimental data that confirm this prediction. The reason for the apparently constant ferrite volume fraction is that the arrest of ferrite growth is triggered by the impingement of the carbon concentration profiles and the associated rapid decrease in velocity. Using the Zener approximation, it is possible to show using a global carbon balance that the impingement of the carbon profiles as a function of grain size will occur at essentially the same ferrite volume fraction.

V. CONCLUSIONS

We present a new model for the interaction of prototypical alloying elements (a strong carbide former, Mo, and two austenite stabilizers, Mn and Ni) with migrating ferrite-austenite interfaces in alloy steels. The model owes much to and is considered an advance on several previous efforts[8,11] to quantitatively describe this fundamental aspect of microstructure development in steels.

The elements of the new model consist of a multiple discrete-jump approach to the trans-interface transport of substitutional solute, the incorporation of the Gibbs energy dissipation associated with the kinetic interfacial solute profiles, and the assignment of a temperature-independent binding energy of each of the solutes to the interface. The frequencies of diffusive jumps within the interface region are systematically derived from volume diffusion data in the parent phases. The fast-diffusing interstitial carbon is considered to be in local equilibrium at all times.

The challenge for the present model lies in the self-consistent description of recently acquired data on ferrite growth in the decarburization of ternary Fe-C-Mo and Fe-C-Mn alloys over a range of compositions and temperatures as well as the precipitation of proeutectoid ferrite from Fe-C-Ni and Fe-C-Mn austenite. The latter includes a signature quantity, the volume fraction of ferrite formed after extended isothermal reaction.[8,9] This quantity, resulting from a cessation of fast ferrite growth, proved elusive in previous modeling studies. It is shown that the model satisfactorily predicts this quantity, including its dependence on austenite grain size. Of course, once initial growth has ceased, interfacial tie-lines will begin to shift and alloying element diffusion profiles develop in both ferrite and austenite phases, as suggested by References 10, 46. The present model will then no longer apply. Reports of alloying element spikes based on microanalyses of specimens for which initial fast growth has ceased are therefore complementary to the model results discussed here, but they are not directly germane.

The kinetic evidence for spikes "buried in austenite" and their interaction with moving interfaces as reported by Chen and van der Zwaag[21] appear to be consistent with the present model's suggestion of a rapid transition to full local equilibrium in Fe-C-Mn at higher temperatures.

The "adjustable parameters" employed in the current work are the solute binding energy and trans-interface diffusivity. However, the requirement that the characteristics of ferrite growth during decarburization and precipitation in Fe-C-Mn be reproduced places severe limits on the choices of these parameters for that system. Similarly, for Fe-C-Ni and Fe-C-Mo, the range of solute binding energies yielding viable solutions is strongly constrained.

An outcome of the present work is a suggestion for the resolution of a troubling paradox, the reported transition to a long-lived paraequilibrium state with increasing temperature in Fe-C-Mn alloys.[19] It is considered that the accepted thermodynamic database is suspect at these highest temperatures. A suggested revision, consistent with experimental data, that does not materially influence the computed phase equilibria at lower temperatures, is presented in the Appendix.

Another prediction of interest lies in the examination of the variation of the alloying element composition in the parent austenite as a function of time and temperature. The question of the "alloying element spike" in austenite has remained a challenge for more than half a century. Although the present estimates are meant to be qualitative rather than definitive, they suggest that the complete spike will exist only at the highest transformation temperatures and that, in general, growth may occur with only a fractional spike.

We conclude that the present model, while remaining limited in certain aspects (it refers to the motion of planar, "incoherent" interfaces, for example), is able to answer a substantial number of outstanding questions in this long-standing area of research. In particular, the successful prediction of cessation of rapid ferrite growth depends on the incorporation of solute drag and of carbon diffusion field impingement effects.

APPENDIX

The phase equilibria between ferrite and austenite in the Fe-Mn system were experimentally investigated by Triano and McGuire,[42] Hillert,[43] and Srivastava and Kirkaldy.[44] The last authors reported the 95 pct confidence interval of their measurements as ±3 pct. The experimental data are summarized in Figure 12 along with the thermodynamic model due to Huang,[45] which is the basis of the TCFE2 database of Thermo-Calc. It is clear from the comparison that the pioneering treatment of Huang[45] systematically underestimates the solubility of Mn in ferrite at high temperatures. The discrepancy is, arguably, insignificant for most applications. In the present case, however, the difference between the experiments and model predictions at 1095 K (822 °C) is sufficient to change the interpretation of the decarburization data at 1098 K (825 °C); PE is predicted if the description of Reference 45 is used, while LENP would be predicted if one modified the description to fit the experimental data of Srivastava and Kirkaldy[44] at 1095 K (822 °C). We have, therefore, modified the description of Reference 45 in order to produce a better fit of the experimental data as shown by the dashed curves in Figure 12. The modifications were limited to one parameter, namely

$$L(\text{bcc, Fe,Mn:Va}; 0) = 4007.8 - 4.44\, T(\text{k})\, \text{J/mol}$$

This description was used for all calculations on the Fe-Mn-C system in this contribution. A more thorough examination of the thermodynamics, including new experimental data between 1095 K and 1173 K (822 °C and 900 °C), seems necessary in order to reach definitive conclusions as to the operating interfacial conditions during decarburization at high temperatures.
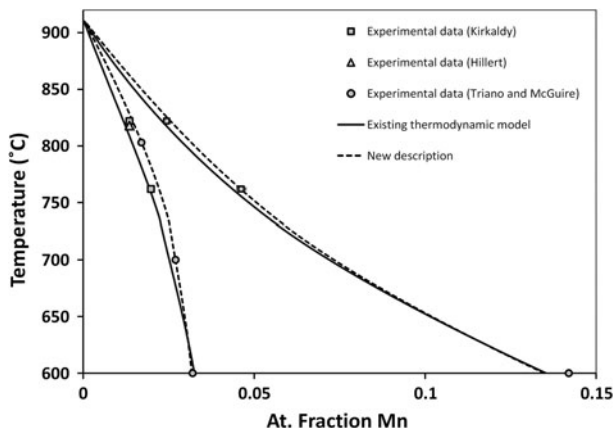

Fig. 12—A portion of the Fe-Mn-C phase diagram. Experimental data point along with the calculated phase boundaries using thermodynamic models by Huang,[45] Srivastava and Kirkaldy[44] and the modified version of Huang's description.

REFERENCES

1. C. Zener: *J. Appl. Phys.*, 1949, vol. 20, p. 950.
2. J.S. Kirkaldy: *Can. J. Phys.*, 1958, vol. 36, p. 907.
3. M. Hillert: "Paraequilibrium," Report of the Swedish Institute for Metal Research, Stockholm, Sweden, 1953.
4. G.R. Purdy, D.H. Weichert, and J.S. Kirkaldy: *Trans AIME*, 1964, vol. 230, p. 1025.
5. D.E. Coates: *Metall. Trans.*, 1972, vol. 3, p. 1203.
6. A. Hultgren: *Trans. ASM*, 1947, vol. 39, p. 915.
7. J.B. Gilmour, G.R. Purdy, and J.S. Kirkaldy: *Metall. Trans.*, 1972, vol. 3, p. 3213.
8. C.R. Hutchinson, A. Fuchsmann, and Y. Brechet: *Metall. Mater. Trans. A*, 2004, vol. 35A, p. 1221.
9. K. Oi, C. Lux, and G.R. Purdy: *Acta Mater.*, 2000, vol. 48, p. 2147.
10. H. Guo, G.R. Purdy, M. Enomoto, and H.I. Aaronson: *Metall. Mater. Trans. A*, 2006, vol. 37A, p. 1721.
11. J. Odqvist, M. Hillert, and J. Agren: *Acta Mater.*, 2002, vol. 50, p. 3211.
12. M. Hillert and B. Sundman: *Acta Metall.*, 1977, vol. 24, p. 731.
13. H. Guo and M. Enomoto: *Metall. Mater. Trans. A*, 2007, vol. 38A, p. 1152.
14. A. Viardin, B. Appolaire, E. Aeby-Gautier, and M. Gouneʹ: Presentation at ALEMI, Avignon, 2010.
15. A. Phillion, H.S. Zurob, C.R. Hutchinson, H. Guo, D.V. Malakhov, J. Nakano, and G. Purdy: *Metall. Mater. Trans. A*, 2004, vol. 35A, pp. 1237–42.
16. C.R. Hutchinson, H.S. Zurob, and Y. Bréchet: *Metall. Mater. Trans. A*, 2006, vol. 37A, p. 1711.
17. H.S. Zurob, C.R. Hutchinson, Y. Bréchet, H. Seyedrezai, and G.R. Purdy: *Acta Mater.*, 2009, vol. 57, p. 2781.
18. H.S. Zurob, C.R. Hutchinson, A. Béché, G.R. Purdy, and Y.J.M. Bréchet: *Acta Mater.*, 2008, vol. 56, p. 2203.
19. H.S. Zurob, C.R. Hutchinson, Y. Bréchet, and G.R. Purdy: *Solid–Solid Phase Transformations in Inorganic Materials 2005*, TMS, Warrendale, 2005, p. 111.
20. H. Chen and S. van der Zwaag: *J. Mater. Sci.*, 2011, vol. 46, p. 649.
21. H. Chen and S. van der Zwaag: *Phil. Mag. Lett.*, 2012, vol. 92, p. 86.
22. J.W. Cahn: *Acta Metall.*, 1962, vol. 10, p. 789.
23. M. Hillert: *Acta Mater.*, 1999, Vol. 47, p. 4481.
24. G.R. Purdy and Y.J.M. Bréchet: *Acta Metall. Mater.*, 1995, vol. 43, p. 3763.
25. K.Lücke and H.P. Stüwe: *Acta Metall.*, 1971, vol. 19, p. 1087.
26. G.R. Purdy: Ph.D. Thesis, McMaster University, Canada, 1962.
27. M. Hillert: *Proceedings ICSTIS, Suppl. Trans. ISIJ*, 1971, vol. 11, p. 1153.
28. H. Oikawa, J.-F. Remy, and A.G. Guy: *Trans. ASM1968*, vol. 61, p. 110.
29. B. Sundman, B. Jansson, and J.O Andersson: *CALPHAD*, 1985, vol. 9, p. 153.
30. J. Agren: *Acta Metall.*, 1986, vol. 20, p. 1507.
31. A. Béché, H.S. Zurob, and C.R. Hutchinson: *Metall. Mater. Trans. A*, 2007, vol. 38A, p. 2950.
32. M. Hillert: in *Lectures on the Theory of Phase Transformation*, H.I Aaronson, ed., TMS, Warrendale, PA, 1999, p. 1–33.
33. C. Sinclair, C.R. Hutchinson, and Y. Bréchet: *Metall. Mater. Trans. A*, 2007, vol. 38A, p. 821.
34. Z.K. Liu: *Metall. Mater. Trans. A*, 1997, vol. 28A, p. 1625.
35. F. Fazeli and M. Militzer: *Metall. Mater. Trans. A*, 2006, vol. 36A, p. 1395.
36. M. Suehiro, Z.K Liu, and J. Agren: *Acta Mater.*, 1996, vol. 44, p. 4241.
37. H. Larsson and A. Borgenstam: *Scripta Mater.*, 2007, vol. 56, p. 61.

38. P. Maugis and G. Martin: *Phys. Rev. B: Condens. Matter Mater. Phys.*, 1994, vol. 49, p. 11580.
39. P. Bellon and G. Martin: *Phys. Rev. B: Condens. Matter Mater. Phys.*, 2002, vol. 66, p. 1.
40. C. Qiu, H.S. Zurob, D. Panahi, Y.J.M. Bréchet, G.R. Purdy, and C.R. Hutchinson: unpublished research.
41. M. Gouné: private communications.
42. A.R. Troiano and F.T. McGuire: *Trans. Am. Soc. Met.*, 1943, vol. 31, p. 340.
43. M. Hillert, T. Wada, and H. Wada: *JISI*, 1967, vol. 205, p. 539.
44. K.K. Srivastava and J.S. Kirkaldy: *Metall. Trans. A*, 1982, vol. 13A, p. 2113.
45. W. Huang: *Metall. Trans. A*, 1990, vol. 21A, p. 2115.
46. H. Guo and G.R. Purdy: *Metall. Mater. Trans. A*, 2008, vol. 39A, p. 950.